

## LETTERS

# Release of volatiles from a possible cryovolcano from near-infrared imaging of Titan

C. Sotin<sup>1</sup>, R. Jaumann<sup>2</sup>, B. J. Buratti<sup>3</sup>, R. H. Brown<sup>4</sup>, R. N. Clark<sup>5</sup>, L. A. Soderblom<sup>6</sup>, K. H. Baines<sup>3</sup>, G. Bellucci<sup>7</sup>, J.-P. Bibring<sup>8</sup>, F. Capaccioni<sup>9</sup>, P. Cerroni<sup>9</sup>, M. Combes<sup>10</sup>, A. Coradini<sup>7</sup>, D. P. Cruikshank<sup>11</sup>, P. Drossart<sup>10</sup>, V. Formisano<sup>7</sup>, Y. Langevin<sup>8</sup>, D. L. Matson<sup>3</sup>, T. B. McCord<sup>12</sup>, R. M. Nelson<sup>3</sup>, P. D. Nicholson<sup>13</sup>, B. Sicardy<sup>10</sup>, S. LeMouelic<sup>1</sup>, S. Rodriguez<sup>1</sup>, K. Stephan<sup>2</sup> & C. K. Scholz<sup>2</sup>

Titan is the only satellite in our Solar System with a dense atmosphere. The surface pressure is 1.5 bar (ref. 1) and, similar to the Earth, N<sub>2</sub> is the main component of the atmosphere. Methane is the second most important component<sup>2</sup>, but it is photodissociated on a timescale of 10<sup>7</sup> years (ref. 3). This short timescale has led to the suggestion that Titan may possess a surface or subsurface reservoir of hydrocarbons<sup>4,5</sup> to replenish the atmosphere. Here we report near-infrared images of Titan obtained on 26 October 2004 by the Cassini spacecraft. The images show that a widespread methane ocean does not exist; subtle albedo variations instead suggest topographical variations, as would be expected for a more solid (perhaps icy) surface. We also find a circular structure ~30 km in diameter that does not resemble any features seen on other icy satellites. We propose that the structure is a dome formed by upwelling icy plumes that release methane into Titan's atmosphere.

Following the exploration of the jovian system by the Galileo spacecraft, the NASA-ESA-ASI Cassini-Huygens spacecraft went into

orbit in Saturn's system on 1 July 2004. Its mission is devoted to observations of Saturn's atmosphere, rings and satellites. Titan, Saturn's largest satellite, has global characteristics similar to the largest galilean satellites Ganymede and Callisto<sup>6</sup>, which do not have atmospheres. The origin, composition, dynamics and evolution of Titan's atmosphere are key questions to be addressed by the Cassini-Huygens mission.

Scattering by haze particles in Titan's atmosphere makes observation of Titan's surface in the visible very difficult, though it can be easily studied in some narrow infrared windows between the numerous methane absorptions<sup>7</sup>. The Visual and Infrared Mapping Spectrometer (VIMS) instrument, which observes in the 0.35 to 5.2 μm wavelength range, is well positioned to observe Titan's surface<sup>8</sup>. The wavelengths where VIMS has the greatest signal-to-noise ratio while minimizing the effects of scattering by the atmospheric haze are between 2.01 μm and 2.03 μm (Fig. 1), which is one of the seven infrared spectral windows (inset in Fig. 1). The images acquired during this first close fly-by allowed us to build a mosaic showing

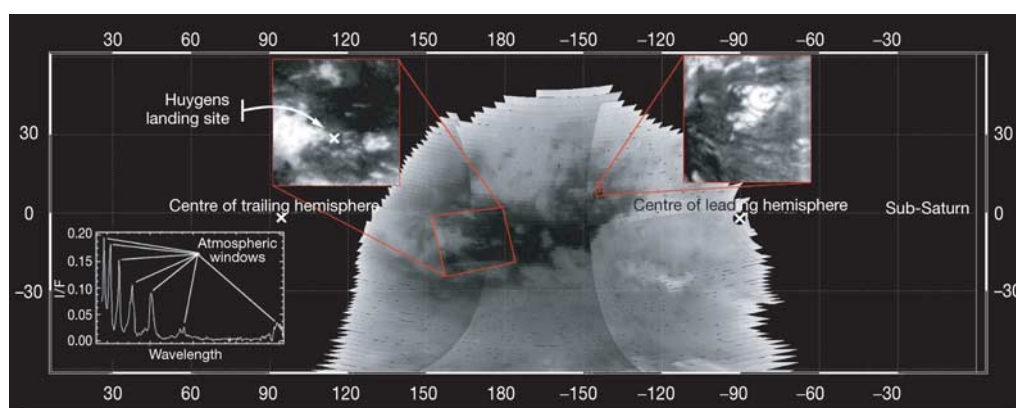


**Figure 1 | Titan's map at 2.03 μm wavelength.** On 26 October 2004, Cassini-Huygens flew over Titan at less than 1,200 km at closest approach, acquiring several hyperspectral images with spatial resolution ranging from a few tens of kilometres to 2 km per pixel. Titan's diameter is 5,151 km, which is larger than Callisto's diameter (4,806 km) but smaller than Ganymede's diameter (5,268 km). Its mean density is 1,881 kg m<sup>-3</sup>, a value between that of rock and that of water. The VIMS instrument took

hyperspectral images from the visible to 5.2 μm wavelength. This figure shows the mosaic obtained at 2.03 μm; horizontal and vertical axes show respectively longitude and latitude in degrees. Observations are centred around the anti-Saturn point. Left inset, high-resolution (30 km pixel<sup>-1</sup>) image, taken to provide the global setting of the site where the Huygens probe successfully landed on 14 January 2005. The best resolved image (right inset) is displayed in Fig. 2.

<sup>1</sup>Laboratoire de Planétologie et Géodynamique, UMR CNRS 6112, Université de Nantes, Nantes, 44100, France. <sup>2</sup>Institute of Planetary Exploration, DLR, Berlin, 12489, Germany.

<sup>3</sup>Jet Propulsion Laboratory, California Institute of Technology, Pasadena, California 91109-8099, USA. <sup>4</sup>Lunar and Planetary Laboratory and Stewart Observatory, University of Arizona, Tucson, Arizona 85721-0092, USA. <sup>5</sup>US Geological Survey, Denver, Colorado 80225, USA. <sup>6</sup>US Geological Survey, Flagstaff, Arizona 86011, USA. <sup>7</sup>Istituto di Fisica dello Spazio Interplanetario, CNR, Rome, 00133, Italy. <sup>8</sup>Institut d'Astrophysique Spatiale, Université de Paris-Sud, Orsay, 91405, France. <sup>9</sup>Istituto di Astrofisica Spaziale e Fisica Cosmica, CNR, Rome, 00133, Italy. <sup>10</sup>Observatoire de Paris, Meudon, 92195, France. <sup>11</sup>NASA Ames Research Center, Moffett Field, California 94035-1000, USA. <sup>12</sup>Department of Earth and Space Sciences, University of Washington, Seattle, Washington 98195-1310, USA. <sup>13</sup>Cornell University, Astronomy Department, Ithaca, New York 14853, USA.

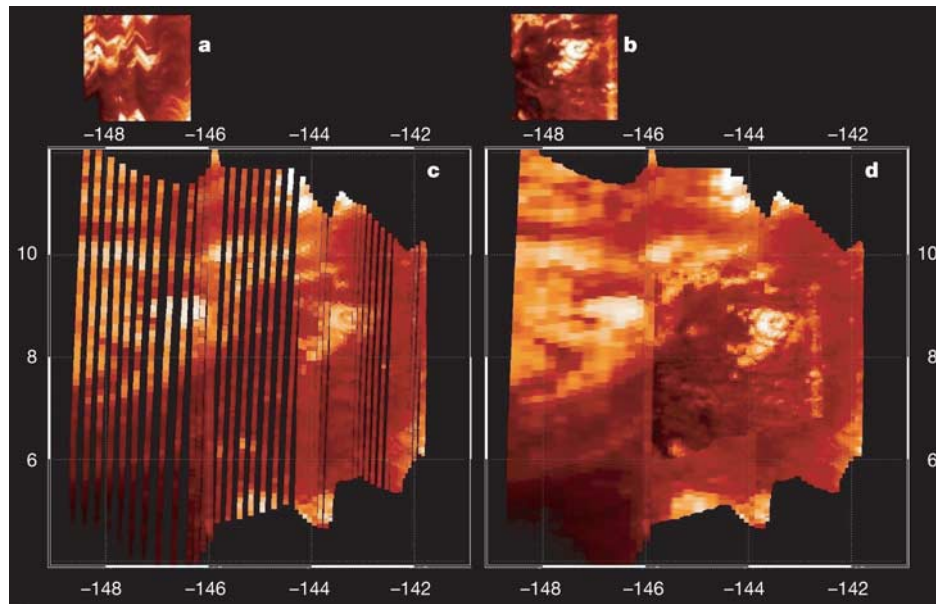


**Figure 2 | VIMS high-resolution observations.** Two high-resolution images were taken during a 25-min period that ended just before closest approach. Because the spacecraft was moving at  $5.8 \text{ km s}^{-1}$  (about  $20,000 \text{ km h}^{-1}$ ) relative to Titan, image motion compensation was required so as to point to the same location on Titan's surface. Two images were acquired of the same area 20 min apart. The non-referenced images are presented in **a** and **b**, and the georeferenced images are presented in **c** and **d**. The first image (**a** and **c**) has a relatively long integration time of 240 ms per pixel. Slight changes in the spacecraft pointing during the observation have distorted the raw image (**a**). Information about Cassini's attitude allowed us to retrieve the exact location of each pixel and to reconstruct the image (**c**). Note that the lines

were not contiguous. The altitude of the spacecraft varied from 11,000 km to about 5,000 km, with a spatial resolution of  $5.5 \text{ km pixel}^{-1}$  to  $3.0 \text{ km pixel}^{-1}$ . The second image was taken with a 80-ms integration, and was centred on the same reference point (**b** and **d**). Because the spacecraft had moved closer to the surface, the resolution varied from  $2.6 \text{ km pixel}^{-1}$  to  $1.8 \text{ km pixel}^{-1}$ . The dominant feature is a bright circular structure ( $8.5^\circ$ ,  $-143.5^\circ$ ) with two elongated wings extending westwards. The short-integration-time image (**d**) is put on top of the long-integration image where interpolation has been performed to fill the gaps between the lines. It allowed us to check that the circular feature has not moved between the two shots.

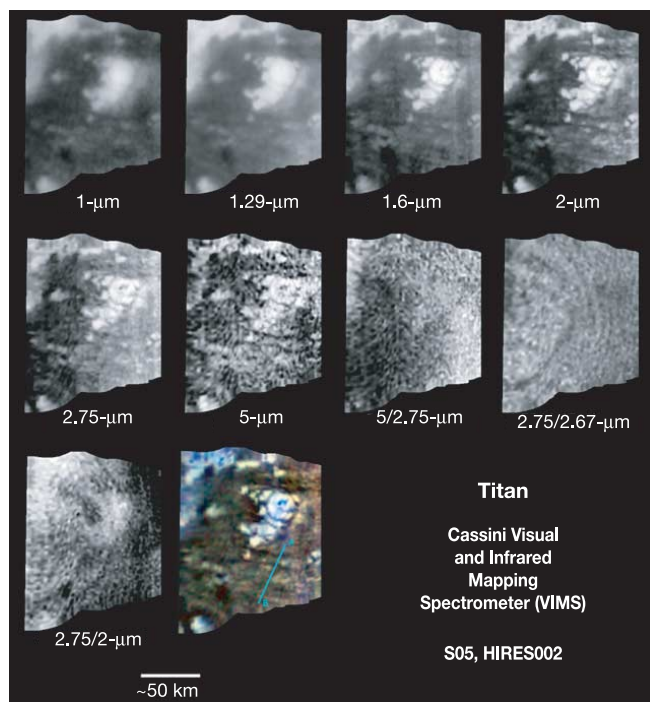


**Figure 3 | High-resolution image of Fig. 2d at different wavelengths.** Details of the circular feature show up at wavelengths larger than  $1.3 \mu\text{m}$ . The first six panels are images taken in six infrared windows (inset in Fig. 1), and are georeferenced. Ratio images are represented in order to visualize compositional variations. The last panel is a colour composite image (red,  $2.75 \mu\text{m}$ ; green,  $2.0 \mu\text{m}$ ; blue,  $1.6 \mu\text{m}$ ). On this panel is represented the A–B segment where we perform the topography analysis. This profile crosses east–west lineaments visible in the different images but not in the ratio images.

bright and dark terrains (Fig. 1). A few higher-resolution images, including the Huygens landing site, were obtained as the spacecraft passed closer to Titan.

The highest-resolution image obtained during the 26 October 2004 fly-by of Titan (Fig. 2) covers about  $150 \text{ km} \times 150 \text{ km}$ . To the right of the image is a bright circular feature about 30 km in diameter, with two elongated wings extending westward. Such a structure resembles volcanic edifices with lobate flows, such as those observed on Earth or Venus for example, although the volcanic material is different. Images in all the infrared windows of the highest-resolution image (Fig. 3) are used to infer information on both the composition and the morphology of this area. At  $2.03 \mu\text{m}$  (Fig. 2), the bright regions are about twice as bright as the dark regions, with apparent reflectance (I/F) values of 0.090 and 0.055, respectively. The spectra of both regions look very similar to first order; thus it seems that the bright and dark materials are similar in composition. The window at  $2.78 \mu\text{m}$  is wide, with two peaks (inset in Fig. 1). As this spectral region corresponds to the beginning of a strong  $\text{H}_2\text{O}$  absorption band, the presence of water ice should make the ratio of the  $2.75\text{-}\mu\text{m}$  image to the  $2.67\text{-}\mu\text{m}$  image (Fig. 3) less than 1, which is not observed, indicating that little, if any, pure water ice is exposed. Also, the  $1.9\text{-}\mu\text{m}$  window should be present if absorption is only due to methane. The very strong  $\text{H}_2\text{O}$  absorption band at  $2 \mu\text{m}$  should make the  $2.03\text{-}\mu\text{m}$  signal weaker than at  $1.9 \mu\text{m}$ , which is never the case. These observations suggest that pure  $\text{H}_2\text{O}$  is not dominantly exposed on the surface of the circular feature or the surrounding area.

Information about the morphology can be obtained by comparing images at different wavelengths. If ratio images do not correlate with albedo variations at a given wavelength, the I/F variations at each wavelength are not related to variations in surface composition. One possibility is that these brightness variations are due to illumination of local slopes. In the south of the bright circular feature, the images

at 2  $\mu\text{m}$ , 2.75  $\mu\text{m}$  and 5  $\mu\text{m}$  show east–west linear features that do not show up either in the 5- $\mu\text{m}$ /2.75- $\mu\text{m}$  ratio image, or in the 2.75- $\mu\text{m}$ /2- $\mu\text{m}$  ratio image (Fig. 3). The solar incidence angle is  $\sim 34^\circ$  (the lighting is approximately from the lower left). We interpret the many linear features, oriented approximately east–west and typically 20–50 km in length and 5–10 km in separation, to be ridges and valleys (Fig. 4; see legend for details of the method). The right panels in Fig. 4 show the results of the method of estimating the haze-scattering component along profile A–B (shown in the left panel). The last image in Fig. 3 has had the resultant spectral haze model removed. With the haze subtracted, the topographic modulation can be used to make a rough estimate of slopes and, by integration, of the topographic relief across the ridge and valley complex. These ridges and valleys have a relief of the order of a few hundred metres and slopes of  $\sim 10^\circ$ . If this interpretation is correct, the dark mottled material (Fig. 4) cannot be liquid at a kilometre scale, which is the spatial resolution of this VIMS image.

Because of variations in colour and albedo, the topography in the central part of the bright circular feature cannot be estimated in this way. It is possible that the haze content is not uniform throughout this area (see 1- $\mu\text{m}$  image in Fig. 3). In the centre of the circular feature is a pixel much darker than its surroundings. This pixel is dark in all infrared windows, and suggests a real feature at the surface. Because the illumination comes from the southwest, the difference in brightness can be explained by a depression, thus it is quite tempting to imagine a caldera-like feature in the centre. Circular, darker lineaments also suggest topography.

Finally, we see no obvious evidence for craters on bright or dark areas, meaning that either the surface is very young, or the surface is liquid. The I/F variations seen in the dark mottled material argue strongly against the presence of liquid.

The image of the Huygens landing site (Fig. 1) brings some complementary information. It can first be noted that the bright area has been proven to be at higher elevation than the dark area by the images taken by the Huygens probe during its descent. Within the bright area imaged by the Huygens probe are black lineaments forming a network that has been compared to dry channels. Finally, the landing site, located on the dark area, is not liquid, which confirms the present interpretations.

Several of the features described above suggest that the high-resolution image (Fig. 2) is a zone of extension. The east–west linear features could be interpreted as tectonic features or flow lines. Similar lineaments are found on Ganymede's grooved terrains<sup>9</sup>. Grooved terrains on Ganymede are areas younger than the heavily cratered dark terrains that are thought to result from extension and resurfacing associated with upwelling. If the lineaments on Titan are related to upwelling 'hot ice' and contain contaminants such as hydrocarbons that vaporize as they get closer to the surface, mechanisms similar to those operating for silicate volcanism may produce flows of differentiated ices on Titan that would not be H<sub>2</sub>O-based. It is worth noting that tidal heating is an important heat source within Titan, because of this satellite's large eccentricity<sup>6</sup>. If tidal heating is focused in low-viscosity domains (hot ice in the upwelling plumes) as has been hypothesized for Europa<sup>10</sup>, this energy may help ice melting and gaseous release in the atmosphere.

The curved black lineaments of the bright circular feature may be similar to dendritic structures seen by Huygens. Such structures could have been formed by the large release of methane-producing rains following the eruptions. If these structures are channels, they would have dried out due to the short timescale for photodissociation of methane in the atmosphere.

Finally, the bright region in the 5- $\mu\text{m}$ /2.75- $\mu\text{m}$  ratio image (Fig. 3) could indicate thermal emission, but the temperature cannot be greater than 200 K. Alternatively, the origin of the bright spot could be related to grain size or compositional variations. Precise radiative-transfer modelling of the atmospheric components and retrieval of

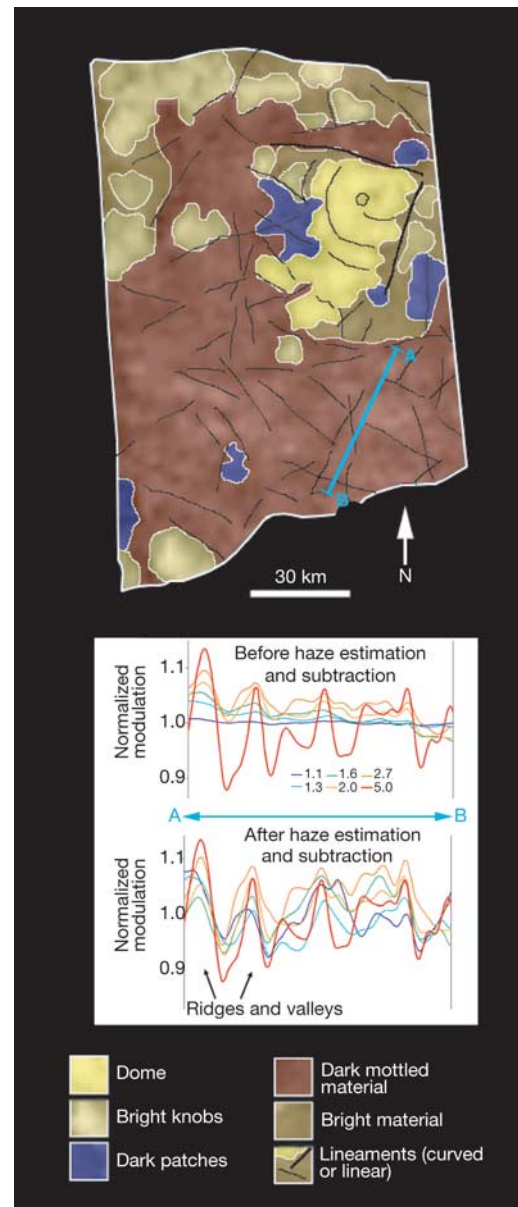


**Figure 4 | Geological interpretation of the high-resolution image.** On the basis of albedo variations and variations in texture, a geological interpretation of the circular feature has been obtained (left panel). Analysis of I/F variations have been realized along profile A–B. The upper panel and the lower panel on the right shows I/F before and after removal of the haze-scattering effect, respectively. Our interpretation of topography rests on several factors: (1) the highest contrast in the topography is in the cross-sun direction; (2) topographic forms have characteristic bilateral symmetry (bright–dark oscillations in the down-sun direction); and (3) after haze removal at shorter wavelengths, the topographic patterns do not correlate in general with variations in spectral reflectance. In addition to geomorphologic interpretation, we can use the topographic modulation to estimate the scattered radiation in each of the spectral windows. We start with three assumptions: first, the scattering haze has a uniform (additive) contribution over the scene at each wavelength; second, the photometric function is approximately independent of wavelength; and third (most important), the atmospheric scattering at 5.0  $\mu\text{m}$  is zero. Also, a lambertian surface is assumed. Scattering effectively dilutes the topographic modulation. If there were no scattering haze, the topographic modulation (that is, that observed at 5.0  $\mu\text{m}$ ) would be the same at all wavelengths. We thereby simply solve for the scattering at each wavelength, which, when subtracted, yields a uniform topographic modulation with wavelength.



surface reflectance are required to distinguish between these different options.

Are there alternative explanations for this bright circular feature? One could imagine that it is a cloud. But there are several arguments against this hypothesis. First, the spectra differ from those already observed for the cloud seen during Cassini's T0 fly-by near Titan's south pole. Second, the two images here (Fig. 2) were taken 20 min apart and no difference can be seen. Third, the Coriolis forces are much smaller on Titan than on Earth owing to Titan's long rotation period (16 days), and circular atmospheric features are not expected at low latitudes.

Another explanation is the accumulation of solid particles transported by gas or liquid, similar to sand dunes on Earth. There is usually a 'V' shape associated with such features, and one could imagine that the bright feature is pointing to the east, with the elongated features representing the tails of the structure. However, the circular shape is difficult to reconcile with such a process. In addition, it would be difficult to explain the dark lineaments with such a structure. Finally, the wind direction in such a case would have to be westward. This is not the direction favoured by current models<sup>11</sup> that predict pole to pole circulation, although the direction of winds in a boundary layer of a dense atmosphere can be different.

We interpret this bright circular feature as a cryovolcanic dome in an area dominated by extension. VIMS is an excellent optical instrument for studying the geology of Titan, as below 1.2  $\mu\text{m}$ , atmospheric scattering dominates, and no surface features show up distinctly. Radar observations of the different sites observed by VIMS during this first close fly-by of Titan will be acquired in the course of the mission. They will provide additional information that will help constrain the tectonic setting of the area described in the present study.

Received 27 December 2004; accepted 24 March 2005.

1. Lellouch, E. Atmospheric model of Titan and Triton. *Ann. Geophys.* **8**, 653–660 (1990).
2. Kuiper, G. P. Titan: a satellite with an atmosphere. *Astrophys. J.* **100**, 329–332 (1944).
3. Yung, Y. L., Allen, M. & Pinto, J. P. Photochemistry of the atmosphere of Titan: comparison between model and observations. *Astrophys. J. Suppl.* **55**, 465–506 (1984).
4. Lunine, J. I. Does Titan have an ocean? A review of current understanding of Titan's surface. *Rev. Geophys.* **31**, 133–149 (1993).
5. Lunine, J. I., Stevenson, D. J. & Yung, Y. L. Ethane ocean on Titan. *Science* **222**, 1229–1230 (1983).
6. Sotin, C. & Tobie, G. Internal structure and dynamics of the large icy satellites. *C.R. Acad. Sci.* **5**, 769–780 (2004).
7. Meier, R., Smith, B. A., Owen, T. C. & Terrile, R. J. The surface of Titan from NICMOS observations with the Hubble Space Telescope. *Icarus* **145**, 462–473 (2000).
8. Brown, B. *et al.* Observations with the Visual and Infrared Mapping Spectrometer (VIMS) during Cassini's flyby of Jupiter. *Icarus* **164**, 461–470 (2003).
9. Lucchita, B. K. Grooved terrains on Ganymede. *Icarus* **44**, 481–501 (1980).
10. Sotin, C., Head, J. W. & Tobie, G. Europa: Tidal heating of upwelling thermal plumes and the origin of lenticulae and chaos melting. *Geophys. Res. Lett.* **29**(8), doi:10.1029/2001GL013844 (2002).
11. Gibbard, S. G. *et al.* Titan's 2- $\mu\text{m}$  surface albedo and haze optical depth in 1996–2004. *Geophys. Res. Lett.* **31**, doi:10.1029/2004GL019803 (2004).

**Acknowledgements** We thank E. Mercier, D. Mège, J.-P. Combe and O. Bourgeois for discussions about interpreting the high-resolution image, and R. Wagner for help in the projection of the cubes.

**Author Information** Reprints and permissions information is available at [npg.nature.com/reprintsandpermissions](http://npg.nature.com/reprintsandpermissions). The authors declare no competing financial interests. Correspondence and requests for materials should be addressed to C.S. (Christophe.Sotin@univ-nantes.fr).